






Investigation of Quasi-particle Relaxation in Strongly Disordered Superconductor Resonators

Jie Hu¹ , Jean-Marc Matin¹ , Paul Nicaise¹ , Faouzi Boussaha¹ , Christine Chaumont¹, Michel Piat², Pham Viet Dung² and Piercarlo Bonifacio³ 

¹ GEPI, Observatoire de Paris, Université PSL, CNRS, 75014 Paris, France

² Université de Paris, CNRS, Astroparticule et Cosmologie, F-75013 Paris, France

³ GEPI, Observatoire de Paris, Université PSL, CNRS, 92195 Meudon, France

E-mail: jie.hu@obspm.fr

December, 2023

Abstract. In this paper, we investigate the quasi-particle (QP) relaxation of strongly disordered superconducting resonators under optical illumination at different bath temperatures with the Rothwarf and Taylor equations and the gap-broadening theory described by the Usadel equation. The analysis is validated with various single-photon responses of Titanium Nitride (TiN) microwave kinetic inductance detectors (MKIDs) under pulsed 405 nm laser illumination. The QP relaxation in TiN is dominated by QPs with energy below the energy gap smeared by the disorder, and its duration is still inversely proportional to the QP density. The QP lifetime versus temperature can be fitted. The relaxation of the resonator can be further modeled with QP diffusion. The fitted QP diffusion coefficient of TiN is significantly smaller than expected. Our result also shows a significant increase in QP generation efficiency as the bath temperature increases.

1. Introduction

Strongly disordered superconductors have been widely used for superconducting resonators for photon detection in astrophysics[1, 2, 3, 4] and qubit readout in quantum circuits[5]. They are particularly favored for microwave kinetic inductance detectors[6] (MKIDs) in the optical and near-infrared bands because of their high quality and high resistivity for better optical efficiency[2, 7, 8].

Compared to aluminum superconducting resonators[9], MKIDs made of strongly disordered superconductors show a different QP relaxation process under optical illumination. First, the QP relaxation in these MKIDs shows a very fast QP relaxation after photon absorption as the bath temperature (T_{bath}) decreases[2, 7, 8, 10]. Second, their resonance frequency shift versus T_{bath} is proportional to the optical power (P_{opt}) under steady illumination[3, 11], while the resonance frequency of MKIDs made of superconductor described by BCS theory[12] is proportional to[9] $\sqrt{P_{opt}}$. Third, the

response in the optical band is much smaller than expected[8, 13, 14]. Fourth, the density of states (DoS) of the QPs below the energy gap (Δ) is not zero due to the energy gap being smeared by the disorder[15]. Thus, many QPs with energy less than Δ would be in the disordered superconductors. However, the response of these QPs to the optical illumination remains unknown.

In this paper, we investigate the QP relaxation time in strongly disordered superconductors with the single-photon response of TiN MKIDs at 405 nm. We show that the QP relaxation in TiN under optical illumination at low temperatures still follows the Rothwarf and Taylor (RT) equations[16] despite the observed anomalous response. We have also obtained an analytical solution of RT equations for superconductors with relatively slow relaxation at low temperatures with various phonon-trapping factors. We further considered QP diffusion in the superconductor and fitted the diffusion coefficient (D_{qp}) and the pair-breaking coefficient (η), showing there is a significant increase in η as the bath temperature increases, which can be the reason for the increasing responsivity of TiN under illumination observed elsewhere[13]. The fitted D_{qp} is significantly smaller than expected, which can be why the QPs relax quickly after the photon absorption.

MKIDs in the optical and near-infrared bands are usually high-quality lumped superconducting resonators[7, 10, 17, 18, 19, 20] that are made of an interdigitated capacitor (IDC) and a meander. Photons ($\hbar\omega > 2\Delta$) absorbed in the meander break Cooper pairs and generate QPs, recombining into Cooper pairs and emitting phonons within the QP lifetime. The extra QPs increase the kinetic inductance and lower the resonance frequency. Such a response can be read out in the phase and amplitude of the resonator by a probing tone at the resonance frequency.

2. Superconducting Gap Broadening

The gap broadening of disorder superconductors is formulated by the Usadel equations as[15, 21, 22]

$$iE \sin \theta + \Delta \cos \theta - \alpha_d \sin \theta \cos \theta = 0, \quad (1)$$

where $\sin \theta$ and $\cos \theta$ are the quasi-classical disorder-averaged Green's functions. E is the energy relative to the Fermi level. The QP DoS can be obtained as $\rho_{qp}(E) = N_0 \text{Re}\{\cos \theta\}$. The case $\alpha_d = 0$ corresponds to the BCS DoS with a peak at $E = \Delta$. When $\alpha_d > 0$, the superconducting gap will be broadened, and there would be nonzero DoS for $E < \Delta$. It means there are QPs with $E < \Delta$. The complex superconductivity $\sigma = \sigma_1 - i\sigma_2$ can be obtained via Nam's theory[23] as

$$\begin{aligned} \frac{\sigma_1}{\sigma_n} = & \frac{1}{\hbar\omega} \int_{E_g - \hbar\omega}^{-E_g} g_1(E, E') [1 - 2f(E')] dE \\ & + \int_{E_g}^{\infty} g_1(E, E') [f(E) - f(E')] dE \end{aligned} \quad (2)$$

$$\begin{aligned} \frac{\sigma_2}{\sigma_n} = & \frac{1}{\hbar\omega} \int_{E_g - \hbar\omega}^{\infty} g_2(E, E') [1 - 2f(E')] dE \\ & + \int_{E_g}^{\infty} g_2(E', E) [1 - 2f(E)] dE, \end{aligned} \quad (3)$$

with g_1 and g_2 as

$$\begin{aligned} g_1 = & \text{Re}\{\cos \theta(E)\} \text{Re}\{\cos \theta(E')\} \\ & + \text{Re}\{\cos \theta(E)\} \text{Re}\{\cos \theta(E')\} \\ g_2 = & \text{Im}\{\cos \theta(E)\} \text{Re}\{\cos \theta(E')\} \\ & + \text{Im}\{i \sin \theta(E)\} \text{Re}\{i \sin \theta(E')\} \end{aligned}$$

$E' = E + \hbar\omega$ and $f(E)$ the Fermi-Dirac distribution, and E_g is the effective energy gap where the DoS starts to be positive and σ_n is the normal-state conductivity, equations 1.3a or 1.3b in [23].

Thus, phonons with energy above $2E_g$ can break the cooper pairs in TiN but with a lower probability.

3. Rothwarf and Taylor Equations

RT equations are a general phenomenological description of the dynamics between QPs and phonons for various superconductors[24, 25, 26, 27, 28] as

$$\begin{aligned} \frac{dn}{dt} = & I + \beta P - Rn^2 \\ \frac{dP}{dt} = & -\frac{\beta}{2}P + \frac{Rn^2}{2} - \gamma(P - P_T^0) \end{aligned} \quad (4)$$

where $n = n(t)$ and $P = P(t)$ are the concentrations of QPs and phonons in the superconductor, $\beta = 2/\tau_B$ is the pair-breaking rate caused by the phonon absorption, τ_B is the time a phonon breaks a cooper pair, and R is the QP recombination rate with the creation of a phonon. I is the background QP generation rate per unit volume. P_T^0 is the concentration of phonons in thermal equilibrium at temperature T with $I = 0$, $\gamma = 1/\tau_{es}$ is their decay rate τ_{es} is the time phonons takes to escape to the substrate. $P_T^0 = Rn_T^2/\beta$ and n_T is the thermally excited QP density as

$$n_T(T) = 4N_0 \int_0^{\infty} f(E, T) \rho(E, T) dE, \quad (5)$$

where $f(E, T)$ is the Fermi-Dirac distribution and $\rho(E, T)$ is the DoS of the QPs. N_0 is the single spin density on the Fermi level. Factor 4 accounts for two possible electronic spins and the integration of DoS from $-\infty$ to ∞ . Here all the phonons with $\hbar\omega > 2E_g$ are taken into account for the broadened superconducting gap. And we still consider that the number of the QP generated by a photon with energy E_{ph} as

$$\delta n = \frac{\eta E_{ph}}{\Delta V}, \quad (6)$$

with η the pair-breaking efficiency and V the volume of the superconductor, as the QP DoS shows a maximum at $E = \Delta$.

By neglecting the spatial fluctuation of the QP density in TiN[29], the steady-state ($dn/dt = 0$ and $dP/dt = 0$) QP density n_{qp} and P_T can be obtained as[30] $n_{qp} = \sqrt{\Gamma I/R + (n_T)^2}$, and $P_T = I/2\gamma + P_T^0$, where $\Gamma = (1 + \beta/2\gamma)$ is the so-called phonon trapping factor[31].

Eq. (4) can be approximated as[26, 27]

$$n(t) = n_1(t) + n_2(t) - n_s \quad (7)$$

n_1 describes the dynamic for the superconductor to reach a quasi-stationary state, in which the QPs density in the superconductor reaches the maximum n_s and starts to recombine back to Cooper pairs. n_2 describes the relatively slow procedure[27] ($d^2n/dt^2 \ll dn/dt$) in which the superconductor recovers from the perturbation. At low temperatures ($T \ll T_c$, T_c is the critical temperature of the superconductor), n_1 , n_2 and n_s are solved as follows[27]

$$n_1(t) = \frac{\beta}{R} \left[-\frac{1}{4} - \frac{1}{2\xi} + \frac{1}{\xi} \frac{1}{1 - \text{Kexp}(-\beta t/\xi)} \right] \quad (8)$$

$$n_2(t) = n_{qp} \left(\frac{1 + \kappa e^{-t/\tau_{qp}}}{1 - \kappa e^{-t/\tau_{qp}}} \right) \quad (9)$$

$$n_s = \frac{\beta}{4R} \left(\frac{2}{\xi} - 1 \right) \quad (10)$$

with the QP relaxation time τ_{qp} as

$$\tau_{qp} = \Gamma/(2n_{qp}R), \quad (11)$$

and

$$\frac{1}{\xi} = \sqrt{\frac{1}{4} + \frac{2R}{\beta}(n_0 + 2P_0)} \quad (12)$$

$$K = \frac{(4Rn_0/\beta + 1) - 2\xi^{-1}}{(4Rn_0/\beta + 1) + 2\xi^{-1}} \quad (13)$$

$\kappa = (n_s - n_{qp})/(n_s + n_{qp}) < 1$ represents the magnitude of perturbation of the QP density in the superconductor.

$n_0 = n_{qp} + \delta n$ and $\delta n = \eta E_{ph}/V \Delta$ is the change of the initial QP density with E_{ph} the photon energy, η the pair-breaking efficiency and V the volume of the superconductor. P_0 is the initial phonon density as

$$P_0 = P_T + \frac{\delta P}{1 + 2\gamma/\beta} \quad (14)$$

where δP is the initial change of the phonon density. We introduce a factor $(1 + 2\gamma/\beta)$ to account for the phonon loss when QP density reaches the maximum. $\delta P > 0$

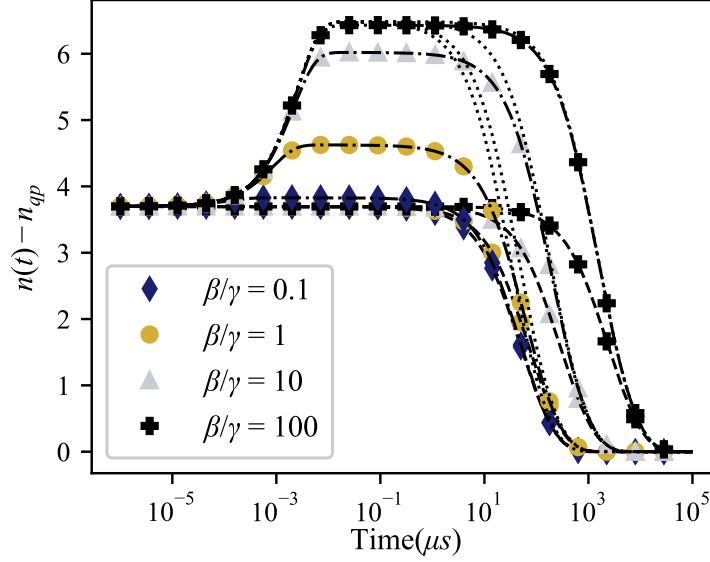


Figure 1. Analytical solution of Eq. (4) at low temperatures. (---), (---) and (.....) corresponds to $\delta P = 0$, $\delta P = (1 - \eta)E/2V\Delta$ and $P_0 = P_T + \delta P$ after initial photon absorption. $P_0 = P_T + \delta P$ corresponds to $\gamma/\beta = 0$, which is referred as strong bottleneck condition[27]. This condition is usually not met for superconductors at extremely low temperatures.

will lead to an increase in QP density after photon absorption[26]. Eq. (9) shares the same expression by Wang et al[32] (Eq. (2)), but with a different meaning of κ . Eq. (9)-(14) are valid for different phonon trapping factors and are compared with the numerical solution of Eq. (4), which are shown in Fig. 1. Here the case with $\delta P = 0$, $\delta P = (1 - \eta)E_{ph}/(2V\Delta)$ with $\eta = 0.57$ are compared, which is a typical value for Cooper-pair breaking detectors [33], primarily constrained by the fact that phonons will not further break Cooper pairs when their energy is less than the binding energy of the Cooper pairs.. The situation $\gamma/\beta = 0$, which corresponds to the original condition[27] for Eq. (7) to (11) is also included for comparison. This condition is usually not met for superconductors at extremely low temperatures as τ_B is relatively long. The QP density increases after photon absorption for $\delta P > 0$, as observed in MgB_2 [26]. Here, we set $\delta P = 0$ for simplicity mainly for two reasons. First, after the superconductor absorbs a photon in the optical band, the created phonons with energy more significant than the Debye energy will escape to the substrate immediately[18]. Second, the response time of MKIDs $\tau_{res} = Q/\pi f_r$ is on the order of $1 \mu\text{s}$, where Q is the quality of the resonator, f_r is the resonance frequency. Thus, it is difficult to determine the value of δP from pulse relaxation. A separate measurement of a TiN film with femtosecond spectroscopy[26] is necessary to determine the value of δP , the recombination rate R , and the pair breaking rate β .

4. MKIDs Transient Response

As the current distribution in the meander is almost uniform, the first-order time-dependent phase response of the MKID $\delta\phi$ relative to the center of its resonance circle on the IQ plane is the convolution[34, 35, 36] between the detector response and the QP's temporal and spatial relaxation $n(x, t)$, which is

$$\delta\phi = \int_0^t \int_V \frac{\phi_0}{\tau_{res}} e^{-(t-\tau)/\tau_{res}} \delta n(v, \tau) dv d\tau, \quad (15)$$

$$\phi_0 = \frac{2\alpha Q \hbar \omega}{\pi \Delta_0 V} \cdot \frac{d\sigma_2}{dn_{qp}}, \quad (16)$$

where $\omega = 2\pi f_r$ is the angular frequency, α is the kinetic inductance fraction, Δ_0 is the energy gap of the superconductor at absolute zero, and σ_2 is the imaginary part of the complex conductivity $\sigma = \sigma_1 - j\sigma_2$ of the superconductor. $d\sigma_2/dn_{qp}$ is estimated numerically with Eq. (3) for TiN.

Table 1. Main Parameters for TiN MKIDs

	T_c	d	L_k	ρ_n^*	Q_i	α_d	Q	f_r	α
	(K)	(nm)	(pH/ \square)	($\mu\Omega \cdot \text{cm}$)	(k)	(Δ_0)	(k)	(GHz)	
<i>TiN_{1K}</i>	0.84	60	84	330	9.0	0.12	6.3	3.182	0.98
<i>TiN_{2K}</i>	2.1	15	61	140	18	0.092	13.1	2.625	0.85
<i>TiN_{4K}</i>	4.0	25	30	210	49	0.132	8.7	4.009	0.60

* ρ_n is measured at before the superconducting transition.

For sufficiently large t (usually on the order of $10 - 20 \mu s$, depending on the QP lifetime) after photon absorption, the QPs diffusion can be neglected. By inserting Eq. (7) into Eq. (15), the temporal phase response of the resonator solved analytically is expressed as

$$\delta\phi = 2n_{qp}\phi_0 V \sum_{m=1}^{\infty} \frac{\tau_{qp}\kappa^m}{\tau_{qp} - m\tau_{res}} (e^{-mt/\tau_{qp}} - e^{-t/\tau_{res}}) \quad (17)$$

We neglected the contribution of $n_1(t) - n_s$ as the time scale is on the order of nanoseconds, much shorter than τ_{res} . For $\tau_{res} \ll \tau_{qp}$, Eq. (17) can be further simplified as

$$\delta\phi \approx 2n_{qp}\phi_0 V \left(\frac{\kappa e^{-t/\tau_{qp}}}{1 - \kappa e^{-t/\tau_{qp}}} - \frac{\kappa}{1 - \kappa} e^{-t/\tau_{res}} \right). \quad (18)$$

The first term in Eq. (18) is the same as the result obtained by Fyhrie et al. [37] with an assumption that QP lifetime saturates at low temperatures[38]. Eq. (18) has been

used to fit the relaxation for QP relaxation for different MKIDs[37, 10]. The procedure to obtain Eq. (15) to (18) can be found in Appendix A

τ_{qp} fitted only by exponential decay will decrease when κ increases. For $\kappa \rightarrow 1$, the higher-order terms $\kappa^m e^{-mt/\tau_{qp}}$ in Eq. (17) become dominant because they have a weight of κ^m in the series and lead to faster relaxation of the resonator with a relaxation time of τ_{qp}/m . Thus, the QP relaxation shows a second relaxation at low temperatures when the QP density in the superconductor is low. The resonator follows an exponential decay when κ decreases, as $\kappa \rightarrow 0$, only the first term in the series in Eq. (17) is essential. In this case, the QP relaxation in MKIDs approaches the exponential decay, and the relaxation time fitted from exponential decay will be close τ_{qp} as the temperature rises.

5. MKIDs Characterization

We investigate the QP relaxation in TiN MKIDs with different critical temperatures by fitting the single photon relaxation at $\lambda = 405$ nm. The detailed parameters for TiN MKIDs are listed in Table 1, where d is the TiN film thickness. The TiN films are deposited on sapphire substrates by magnetron sputtering, which are then patterned into resonators using photolithography and reactive ion etching. The films' internal quality factor Q_i is relatively low as they are fabricated on sapphire[13, 14, 39], which is probably due to the lattice mismatch on their interface. The MKIDs design of TiN_{1K} can be found in the Appendix B The design of TiN_{2K} and TiN_{4K} can be found in our previous publication[13].

The MKIDs are characterized in a pulse tube-pre-cooled adiabatic demagnetization refrigerator (ADR)[40]. A niobium cylinder shields the stray magnetic field and sheets of metglas 2714a around MKIDs. A pulsed 405 nm laser illuminates the MKIDs through an optical fiber. The MKIDs are read by a standard homodyne mixing scheme with a readout power of about 2 dB below bifurcation. The pulse response of the MKID is sampled by an oscilloscope at 100 MHz and processed by a Wiener optimal filter to generate the photon-counting statistics with the average pulse phase response as the template. More details on the measurement setup can be found in Appendix C.

The measured height pulse statistics with two different optical illumination powers are shown in the inset of Fig. 2 for TiN_{1K} , in which the first two peaks correspond to 0-photon and 1-photon. We obtain 0-photon and 1-photon responses by averaging the hundreds of events in the full-width-at-half-maximum (FWHM) in the corresponding peaks. The 0-photon event corresponds to a non-zero background phase response that is due to electrical crosstalk from the surrounding pixels, phonons from the surrounding pixels through the substrate, as well as the photon absorbed in the Nb ground plane and the Nb feedline, as its rise time is around $3.5 \mu s$ and is much longer than $\tau_{res} \approx 0.6 \mu s$. The pulse statistics shift towards the right, which indicates a more significant background response. The 0-photon can be reduced using a microlens array[2] above the meander or continuous illumination[18]. We used a pulsed illumination as it better captures the pulse response's rising edge and the multi-photon events.

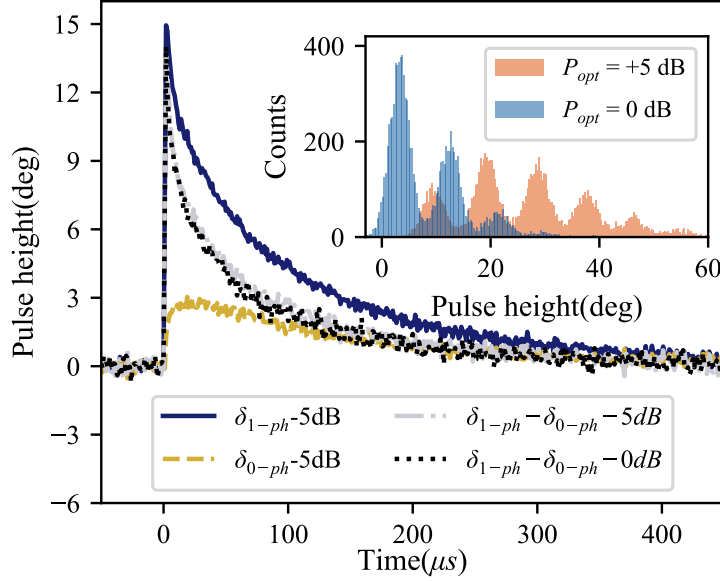


Figure 2. The 1-photon and the 0-photon responses averaged from the FWHM of the corresponding peak in the pulse statistics of the measured MKID for $P_{opt} = 5$ dBm. The photon absorption in the meander is obtained by removing the 0-photon event calculated by Eq. (19). The inset shows the pulse statistics illuminated with two different optical powers.

Due to the high resistivity of the TiN film, the diffusion length of the QPs $l = \sqrt{D_{qp}\tau_{qp}}$ is much shorter than the total length of the meander, as the QP diffusion coefficient[41] is $D_{qp} = D_N \sqrt{2k_B T / \pi \Delta}$, with $D_N = \sigma_n / e^2 N_0$, σ_n the normal state conductivity. Therefore, the 0-photon and the photon absorption in the meander can be considered independent. The 1-photon response $(\delta I_1, \delta Q_1)$ can be decomposed as the summation of the 0-photon response $(\delta I_0, \delta Q_0)$ and the photon absorption $(\delta I_{ph}, \delta Q_{ph})$ in the meander in the in-phase and quadrature plane as

$$\delta I_1 = \delta I_0 + \delta I_{ph}, \quad \delta Q = \delta Q_0 + \delta Q_{ph}. \quad (19)$$

After removing δI_0 and δQ_0 , the phase response of the photon absorption can be calculated, as shown in Fig. 2, which has a shorter relaxation time than the 0-photon response and a very fast relaxation after the photon absorption. And they are the same for the two optical powers.

We fit the resonance frequency shift $\delta f_r / f_r$ and the QP relaxation time τ_{qp} versus T_{bath} together with the superconducting gap broadening with the disorder to obtain Γ / R , α_d , the measure of the disorder of the superconductor and a parameter to calculate the DoS of the QPs in TiN, I , the background QP generation rate in Eq.(4) and T_{qp} , the temperature of the QPs. The resonance frequency shift based on the Mattis-Bardeen theory[42] is added for comparison. The resonance frequency versus the T_{bath} can be fitted as[43] $\delta f_r / f_r = \alpha \delta \sigma_2 / 2\sigma_2$ for thin film, as shown in Fig. 3-(A). The inset shows the broadened DoS at $T = T_c$. The QP lifetime shown in Fig. 3-(B) is fitted with

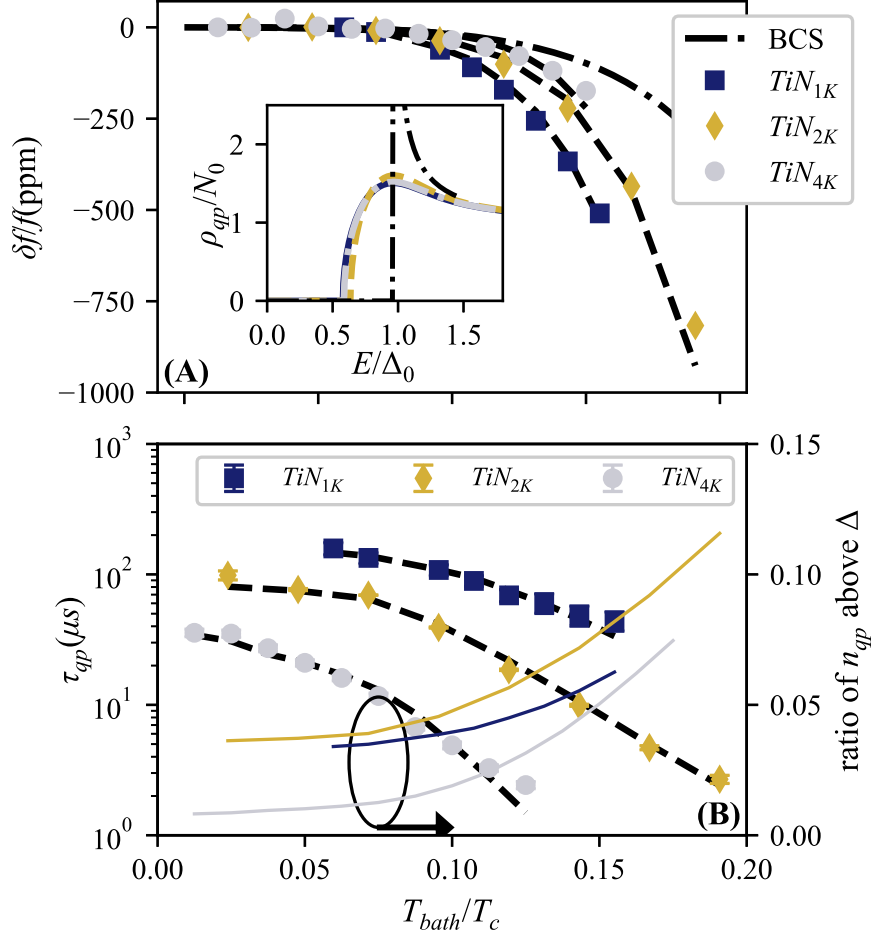


Figure 3. (A): Measured frequency shift versus T_{bath}/T_c for different MKIDs as shown in Table 1. The dashed line is the fitted frequency shift with the disorder. The dashed dot line (— · —) is calculated with the standard Mattis Bardeen theory[42]. The inset shows the broadened DoS at $T = 0.1T_c$. The dashed dot line shows the DoS for the BCS superconductor. (B): Fitted QP lifetime with Eq. (17) from the single-photon response of different MKIDs versus T_{bath}/T_c . The dashed line is fitted with $\tau_{qp} = \Gamma/2n_{qp}R$ versus temperature. The right axis shows the ratio of the QPs above Δ in n_{qp} , calculated as $4N_0 \int_{\Delta}^{\infty} f(E, T) \rho(E, T) dE / n_T(T_{qp})$. $n_T(T_{qp})$ is calculated with (5).

phase relaxation starting from the half of the maximum of the pulse response[10] with Eq. (17). Eq. (11) is fitted to the measured values of the QP lifetime versus T_{bath} .

We assume a Kapiza boundary[44] on the interface between the TiN and the sapphire as

$$P_d = \Sigma A_s (T_{qp}^4 - T_{bath}^4), \quad (20)$$

where Σ is a material constant, A_s is the area of the meander and P_d is the dissipated microwave power in the resonator due to the internal loss[45]. T_{bath} refers to the temperature of the sapphire substrate and is considered the same as that of the

thermometer. Here, we neglect the temperature difference between QPs and phonons in the superconductor as we do not observe significant QP lifetime saturation[46, 47]. T_{qp} is expected to be higher than phonon temperature in the superconductor when T_{bath} is low due to the thermal decoupling between the electrons and phonons. The obtained T_{qp} is about 120 mK, 273 mK, and 400 mK for TiN_{1K} , TiN_{2K} and TiN_{4K} respectively at $T_{bath} = 50$ mK. Although the phonon temperature is overestimated, the equivalent temperature of the QPs remains reasonable[48, 46]. It can be seen that Fig. 3-(B) that the QPs with energy less than Δ dominate, and we can also expect that when T_{bath} is low compared to T_c , the QP dynamic of TiN deviates from the BCS theory as the ratio of QPs with energy less than Δ increases. The detailed fitting procedure can be found in the Appendix D.

6. Quasi Particle Diffusion

We further analyze the QP diffusion by introducing the diffusion term in the RT equations as[49]

$$\begin{aligned}\frac{dn}{dt} &= D_{qp} \nabla^2 n + I + \beta P - Rn^2 \\ \frac{dP}{dt} &= D_{ph} \nabla^2 P - \frac{\beta}{2} P + \frac{Rn^2}{2} - \gamma(P - P_T^0)\end{aligned}\quad (21)$$

D_{qp} and D_{ph} are the diffusion coefficients for the QPs and phonons.

It is observed that as long as the QP lifetime τ_{qp} is kept the same, the solution of Eq. (4) will be the same for different Γ . Thus, with the fitted Γ/R , T_{qp} , I and α_d , n_{qp} can be calculated. R can be obtained if we assume a value for β and η . As we don't observe high energy resolving power in our MKIDs, Γ is set to be on the order of 1. We further assume $D_{ph} = 0$ the phonon diffusion is negligible. In this case, by neglecting the process of 2D QP diffusion to 1D after photon absorption, the measured pulse response of MKIDs can be fitted with the result numerically obtained by solving Eq. (4) and (15) in 1D with two fitting parameters, the quasi-particle diffusion coefficient D_{qp} and the pair breaking efficiency η with a proper initial condition.

The initial QPs are assumed to be Gaussian distributed with σ_0 on the order of the thickness of the film. The Gaussian distribution is taken as the QP density should be continuous and symmetrical after the initial photon absorption, and it is a good approximation of the Dirac function. D_{qp} is almost independent of σ_0 , while η shows a strong dependence as the initial relaxation rate of QP after the photon absorption is proportional to n_{qp}^2 . The σ_0 is chosen to have η smaller than 0.6. We consider that τ_{qp} for TiN_{4K} is too short and that the initial 2D QP diffusion is essential. The 1D diffusion model doesn't hold for TiN_{4K} . We fix[50] $N_0 = 6.0 \times 10^{10} \text{ eV}^{-1} \mu\text{m}^{-3}$, a value needed to be determined experimentally for our film by measuring the diffusion constant in the normal state. The detailed fitting procedure can be found in Appendix E.

The single photon response fitted with Eq. (4) and (15) is shown in Fig. (4)-(A) for TiN_{1K} and TiN_{2K} at $T_{bath} = 50$ mK, which shows that the fast QP relaxation term

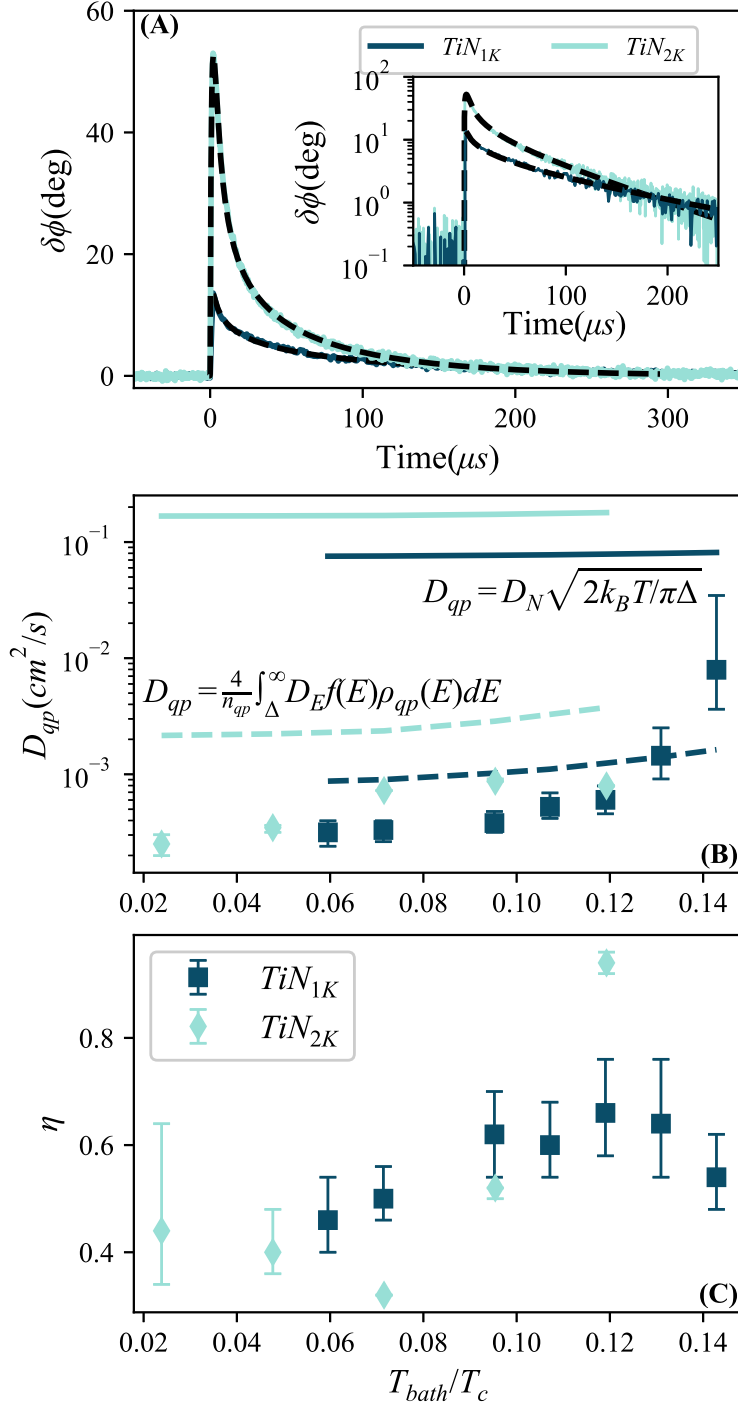


Figure 4. (A): Measured and fitted resonator relaxation for TiN_{1K} and TiN_{2K} at $T_{bath} = 50$ mK with 1-D diffusive RT equations. The inset shows the pulse in the log scale. (B): The fitted diffusion coefficient versus normalized temperature. The solid line is calculated as $D_{qp} = D_N \sqrt{2k_B T / \pi \Delta}$. The dashed line is calculated as $D_{qp} = \frac{4}{n_{qp}} \int_{\Delta}^{\infty} D_E f(E) \rho_{qp}(E) dE$. (C) The fitted photon to QP conversion efficiency η at different temperatures. The error bar corresponds to one standard deviation σ and is obtained when χ^2 increases by about 2.3, corresponding to σ for two parameter fitting.

can be well modeled.

The fitted D_{qp} versus T_{bath} is shown in Fig. (4)-(B). It is about two orders smaller than the theoretical value for two reasons. First, we have considered the QPs with energy less than Δ and still assume the QP density follows the Fermi-Dirac distribution. The number of these QPs significantly outnumbered the QPs with $E > \Delta$, as is shown in Fig. 3-(B). The diffusion coefficient of the QPs is energy-dependent, such as for the BCS superconductor[51],

$$D_E = D_N \sqrt{1 - (\Delta/E)^2}. \quad (22)$$

Thus, the diffusion coefficient of the low-energy QPs should be significantly lower than those with energy larger than Δ . Second, there is a spatial distribution of the Δ in the TiN[52], which makes the QPs more difficult to diffuse. The D_{qp} we obtained can be interpreted as the average D_{qp} over the QPs with different energy. As QP diffusion dispersion is not known for TiN, Eq. (22) is taken for calculation. Then, the averaged diffusion coefficient can be calculated as

$$D_{qp} = \frac{4}{n_{qp}} \int_{\Delta}^{\infty} D_E f(E) \rho_{qp}(E) dE, \quad (23)$$

which is in qualitative agreement with the fitted QP diffusion coefficient. Essentially, we treat the QPs with $E < \Delta$ as "trapped" QPs, which are consistent with the arguments for the anomalous response in TiN[7, 3].

A direct measurement of the QP diffusion coefficient of TiN at low temperatures is needed to investigate the diffusion coefficient further. The low diffusion coefficient can be the reason for the response of the MKIDs made of disordered superconductors being small[13, 14].

We focus on how η evolves with T_{bath} in Fig. 4-(C). η tends to increase when T_{bath} increases especially for TiN_{2K} . One of the possible reasons for the rise of η is due to the presence of the two-level system (TLS) on the interface between the TiN and the sapphire, which absorbs part of the photon energy[19]. As T_{bath} increases, TLS saturates, and then η increases. Another possible reason is when the temperature is low, the phonon generated by the recombination of the QPs with energy less than Δ has a lower probability of breaking Cooper pairs. When T_{bath} increases, the percentage of QPs with energy above Δ increases, increasing η . Additionally, an increase in T_{bath} boosts the D_{qp} , resulting in more QPs being detected by the resonator. With the n^2 term influencing the recombination rate in the RT equation, a higher D_{qp} translates to slower QP relaxation. In this case, η will increase as the temperature increases, consistent with the previous publications[3, 13, 14], where an increase of responsivity of the MKIDs has been observed when T_{bath} rises. The fitted η shows large uncertainty as η is mainly related to the maximum of the pulse, which usually shows large uncertainty.

We show how η and D_{qp} affect the response of MKIDs in Fig. 5 and Fig. 6. It can be seen that D_{qp} significantly affects the pulse response.

The increase in η versus T_{bath} could be one of the reasons why the frequency change of TiN MKIDs versus optical illumination is proportional to P_{opt} in the continuous

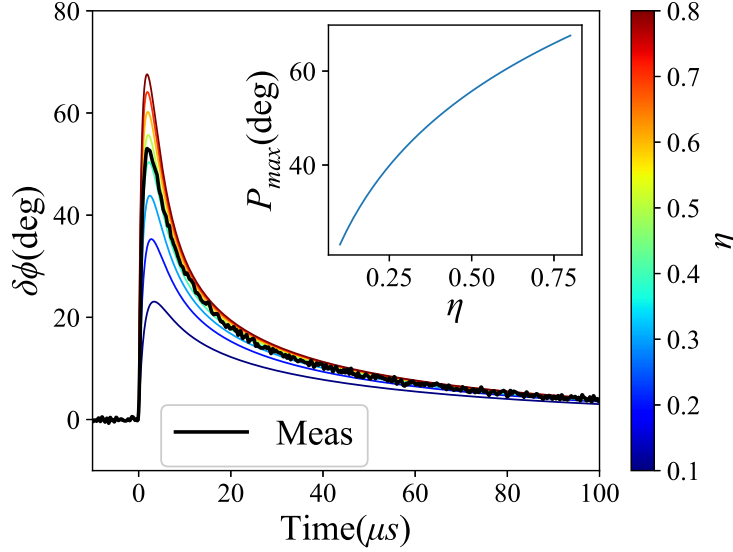


Figure 5. MKIDs response with different η for TiN_{2K} at $T_{bath} = 50$ mK. The inset shows the maximum of the pulse versus η . D_{qp} is fixed with value shown in Fig. 4-(B)

illumination in the millimeter wave range. For the continuous illumination, the change in QPs in the superconductor is $\delta n_{qp} = \eta P_{opt} \tau_{qp} / (\Delta V)$. With Eq. (11), $\tau_{qp} = \Gamma / [2(n_{qp} + \delta n_{qp})R]$. Then, δn_{qp} can be solved as

$$\delta n_{qp} = -\frac{n_{qp}}{2} + \frac{1}{2} \sqrt{n_{qp}^2 + \frac{2\eta(P_{opt})P_{opt}\Gamma}{R\Delta V}}. \quad (24)$$

Here we put η as a function of P_{opt} to indicate its temperature dependence. If η increases with P_{opt} , the responsivity of MKIDs would increase with P_{opt} , as is observed in previous publications[3, 11]. We consider it necessary to solve the full kinetic equations[53] to investigate better the rising edge of the pulse response of MKIDs and better understand the temperature dependence of η .

7. Conclusion

In conclusion, we have modeled the single-photon relaxation process of TiN MKIDs on sapphire with the diffusive Rothwarf and Taylor equations and the gap-broadening theory based on the Usadal equation for disordered superconductors. Our results qualitatively show the QPs with energy less than Δ dominate the QP relaxation. The QP diffusion coefficient leads to fast relaxation of QPs after the photon absorption observed in different materials.

Acknowledgement

The authors would like to thank Damien Prêle and Manuel Gonzalez from APC, Université Paris Cité, for discussion about measurement, as well as Florent Reix, Josiane

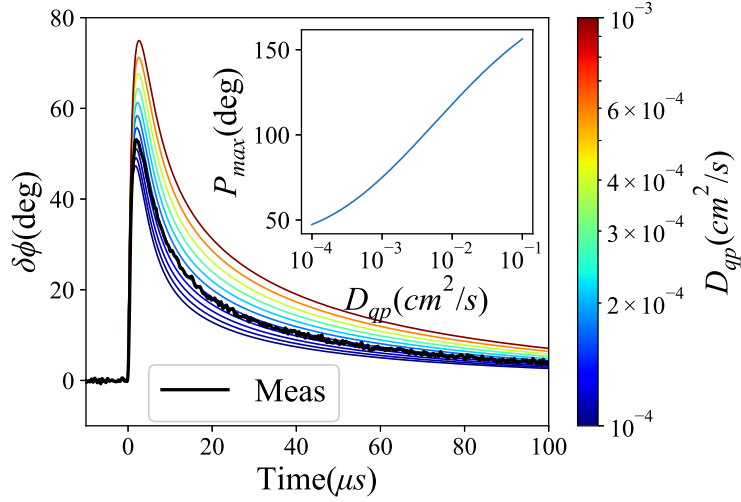


Figure 6. MKIDs response with different D_{qp} for TiN_{2K} at $T_{bath} = 50$ mK. The inset shows the maximum of the pulse versus D_{qp} . η is fixed with value shown in Fig. 4-(C)

Firminy, and Thibaut Vacelet from Paris Observatory for assembly and mounting of the devices. The authors would also like to thank Dr. Eduard Driessen from IRAM and Dr Wei-Tao Lv from the Department of Physics at the Chinese University of Hong Kong for discussing disordered superconductors. This work is supported by the European Research Council (ERC) through Grant 835087 (SPIAKID) and the UnivEarthS Labex program.

Appendix A. MKIDs Responsivity

The response of MKIDs to excess QPs can be expressed as

$$d\phi = \frac{d\phi}{d\omega_r} \cdot \frac{d\omega_r}{dL} \cdot \frac{dL}{d\sigma_2} \cdot \frac{d\sigma_2}{dn_{qp}} \cdot \frac{\delta N_{qp}}{V} \quad (A.1)$$

with[54] $d\phi/d\omega_r$ the change of phase due to the change of the resonance frequency, and $d\omega_r/dL$ the resonance frequency change due to the change of the inductance as

$$\frac{d\phi}{d\omega_r} = \frac{4Q}{\omega_r} \quad (A.2)$$

$$\frac{d\omega_r}{dL} = -\frac{\alpha\omega_r}{2L_k} \quad (A.3)$$

with $L = L_g + L_k$ the total inductance in the resonator, $\alpha = L_k/L$ the fraction of the kinetic inductance and L_g is the geometrical inductance. α is close to 1 for TiN. ω_r is the resonant frequency. For a thin film superconductor, the kinetic inductance is $L_s = 1/(\sigma_2\omega d)$ and d is the film thickness[43], thus,

$$\frac{dL}{d\sigma_2} = -\frac{L_k}{\sigma_2} \quad (A.4)$$

With[43] $\sigma_2/\sigma_n \approx \pi\Delta_0/(\hbar\omega)$ and σ_n the normal state conductivity, Eq. (A.1) can be expressed as

$$d\phi = \frac{2\alpha Q\hbar\omega}{\pi\Delta_0\sigma_n} \cdot \frac{d\sigma_2}{dn_{qp}} \cdot \frac{\delta N_{qp}}{V} \quad (\text{A.5})$$

Here, δN_{qp} is the change of the QP number in the resonator, and it can be expressed as the convolution with the detector response as

$$\delta N_{qp} = \int_0^t \int_V \frac{e^{-(t-\tau)/\tau_{res}}}{\tau_{res}} \delta n(v, \tau) dx d\tau \quad (\text{A.6})$$

where V is the volume of the meander, $\tau_{res} = Q/\pi f_r$ is the response time of the resonator. By substituting Eq. (A.5) into Eq. (A.6), Eq. (15) in the main text can be obtained, as

$$\begin{aligned} \delta\phi &= \int_0^t \int_S \frac{\phi_0}{\tau_{res}} e^{-(t-\tau)/\tau_{res}} \delta n(s, \tau) ds d\tau. \\ \phi_0 &= \frac{2\alpha Q\hbar\omega}{\pi\Delta_0 V} \cdot \frac{d\sigma_2}{dn_{qp}} \end{aligned}$$

For TiN, we calculate the $d\sigma_2/dn_{qp}$ numerically with Eq. (3) in the main text. For a BCS superconductor, $d\sigma_2/dn_{qp}$ can be calculated as

$$\frac{d\sigma_2}{dn_{qp}} = -\sigma_n \frac{\pi S_2}{2N_0\hbar\omega}, \quad (\text{A.7})$$

$$S_2 = 1 + \sqrt{\frac{2\Delta_0}{\pi k_B T}} e^{-\xi} I_0(\xi) \quad (\text{A.8})$$

with $\xi = \hbar\omega/2k_B T$ and I_0 is the Bessel function of the first kind.

For sufficiently large t (usually on the order of 10-20 μs , depending on the QP lifetime) after photon absorption, the spatial distribution of the $\delta n(x, t)$ can be neglected. Thus, with Eq. (9), $\delta n(t)$ can be expressed as

$$\begin{aligned} \delta n(t) &= n_{qp} \left(\frac{1 + \kappa e^{-t/\tau_{qp}}}{1 - \kappa e^{-t/\tau_{qp}}} \right) - n_{qp} \\ &= \frac{2\kappa n_{qp} e^{-t/\tau_{qp}}}{1 - \kappa e^{-t/\tau_{qp}}} \\ &= 2n_{qp} \sum_{m=1}^{\infty} \kappa^m e^{-mt/\tau_{qp}} \end{aligned} \quad (\text{A.9})$$

By substituting Eq. (A.9) into Eq. (15), we obtain Eq. (17) as

$$\begin{aligned} \delta\phi &= \frac{\phi_0 V}{\tau_{res}} \int_0^t e^{-(t-\tau)/\tau_{res}} 2n_{qp} \sum_{m=1}^{\infty} \kappa^m e^{-m\tau/\tau_{qp}} d\tau \\ &= \frac{2n_{qp} V \phi_0}{\tau_{res}} \sum_{m=1}^{\infty} \kappa^m e^{-t/\tau_{res}} \int_0^t e^{-\frac{m\tau}{\tau_{qp}} + \frac{\tau}{\tau_{res}}} d\tau \\ &= 2n_{qp} V \phi_0 \sum_{m=1}^{\infty} \kappa^m \frac{\tau_{qp}}{\tau_{qp} - m\tau_{res}} (e^{-mt/\tau_{qp}} - e^{-t/\tau_{res}}) \end{aligned}$$

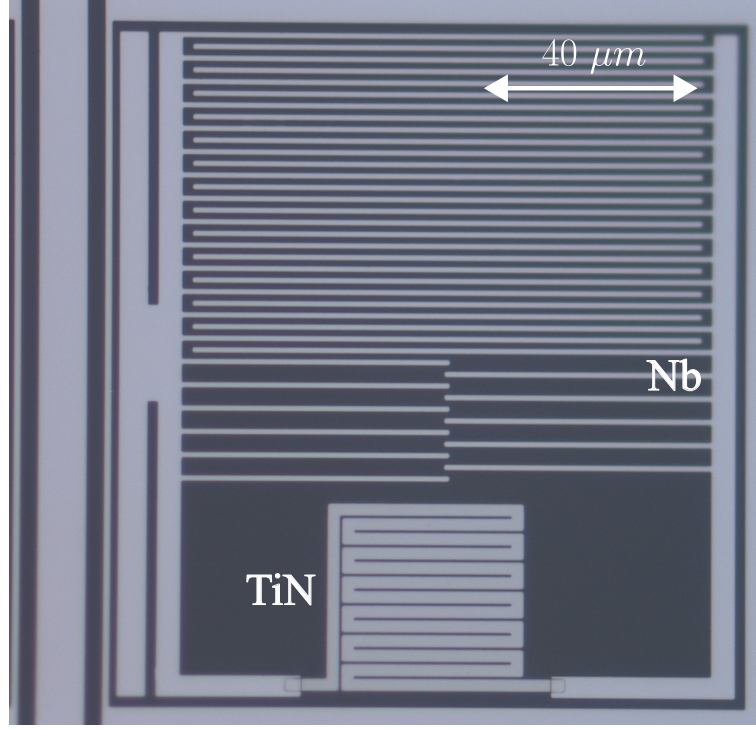


Figure B1. MKIDs design for TiN_{1K} . The meander is made of TiN. The rest of the resonator and the feedline are made of Niobium.

For $\tau_{qp} \gg \tau_{res}$, we obtain Eq. (18) as

$$\begin{aligned} \delta\phi &\approx 2n_{qp}V\phi_0 \sum_{m=1}^{\infty} \kappa^m (e^{-mt/\tau_{qp}} - e^{-t/\tau_{res}}) \\ &= 2n_{qp}V\phi_0 \left(\frac{\kappa e^{-t/\tau_{qp}}}{1 - \kappa e^{-t/\tau_{qp}}} - \frac{\kappa}{1 - \kappa} e^{-t/\tau_{res}} \right) \end{aligned} \quad (\text{A.10})$$

Appendix B. TiN_{1K} MKIDs Design

The detailed design of MKIDs with TiN_{1K} is shown in Fig. B1. The measured TiN MKID is one of the first pixels in a 1000-pixel array. The meander line is made of sputtered 60 nm TiN on sapphire with a film resistivity of about $\rho_n = 330 \mu\Omega \cdot \text{cm}$ ($R_s \approx 55.0 \Omega/\square$) and its size is $40.5 \times 38.5 \mu\text{m}^2$ with a strip width of $2.5 \mu\text{m}$ and a gap of $0.5 \mu\text{m}$. The total length of the meander is about $520 \mu\text{m}$. The IDC is made of niobium, and its size is about $120 \times 90 \mu\text{m}^2$ with both strip width and spacing of $1.2 \mu\text{m}$. The niobium film is 100 nm with a critical temperature of around 9.2 K and a kinetic inductance of about $0.2 \text{ pH}/\square$.

Appendix C. Measurement Setup

The detailed measurement setup for the MKIDs is shown in Fig. C1. The MKIDs are characterized in a two-stage pulse tube pre-cooled adiabatic demagnetization refrigerator

(ADR) at Laboratoire Astroparticule & Cosmologie (APC). The stray magnetic field is shielded by a niobium cylinder that is 1.5 mm thick and sheets of metglas 2714a around MKIDs. The niobium cylinder is thermalized on the 1 K stage and encloses the entire 0.1 K stage. The MKIDs are read by a standard homodyne mixing scheme. The input signal is generated by a signal generator (SMA100A). It is first attenuated by a programmable attenuator (RCDAT-8000-60) at room temperature and then attenuated 20 dB, 10 dB, and 20 dB (XMA-2082 series) on 4 K, 1 K, and 100 mK before being fed into MKIDs. The output signal from MKIDs is first amplified by an LNA (LNF-LNC0.3.14B) on the 4K stage and amplified further by two room temperature amplifiers (ZVA-183W-S+). The signal is down-converted to DC by an IQ mixer (AD(0.4-6.0)) and then sampled by an oscilloscope (HDO6034). Two double DC blocks (SD3463) are placed between the 4K and 1K stages to operate the heat switch in the cryostat. The readout power is estimated to be around -100 dBm at the input of the detector. The MKIDs array is illuminated by an optical fiber placed 35 mm above the pixels. The 405 nm laser (LP405C1) is modulated by a 250 Hz pulse from the pulse generator (TG5012A) of a width of 50 ns. The output power of the laser is estimated to be a few pW outside the cryostat, attenuated by a digital step attenuator (DD-100 series from OZ optics). The pulse response of the MKID is sampled by an oscilloscope (HDO6034) at 100 MHz.

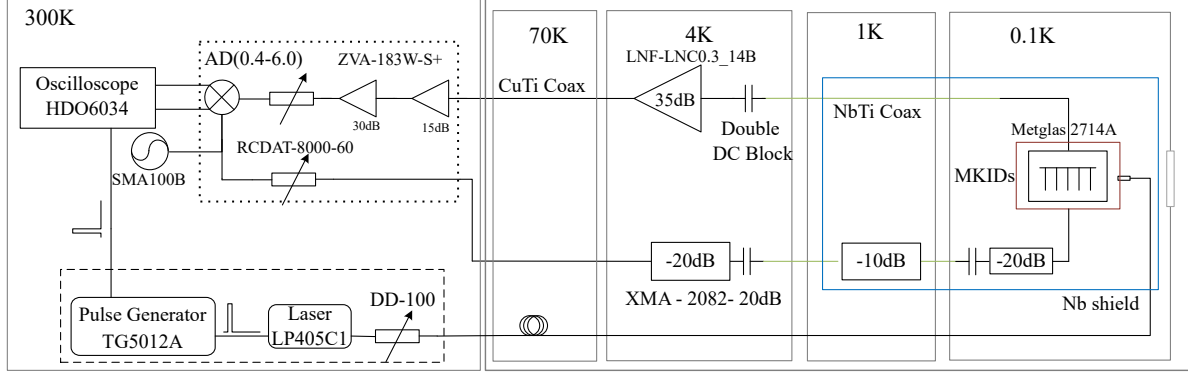


Figure C1. Detailed measurement Setup for the MKIDs

Appendix D. Resonance frequency shift and QP lifetime fitting

We first fit the quality factor Q , resonant frequency f_r and the coupling quality factor Q_c from the transmission of the resonator S_{21} as

$$S_{21} = ae^{-2\pi j f \tau} \left[1 - \frac{Q/Q_c e^{j\phi_0}}{1 + 2jQ(f - f_r)/f_r} \right] \quad (\text{D.1})$$

where a is the amplitude of the transmission. τ is the time delay on the cable. ϕ_0 is the parameter to account for the mismatch of the resonator to the circuit.

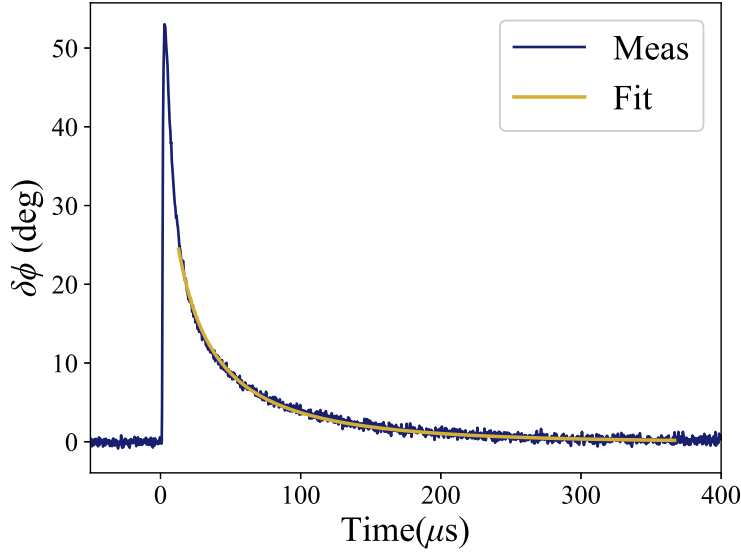


Figure D1. QP lifetime τ_{qp} fitting for TiN_{2K} at $T_{bath} = 50$ mK.

The QP lifetime is fitted from the pulse relaxation from the half of the maximum using Eq. (17) in the main text, which we rewrite here as

$$\delta\phi = 2Vn_{qp}\phi_0\tau_{qp} \sum_{m=1}^{\infty} \frac{\kappa^m}{\tau_{qp} - m\tau_{res}} (e^{-mt/\tau_{qp}} - e^{-t/\tau_{res}}).$$

We show an example of fitting the QP lifetime τ_{qp} for TiN_{2K} at $T_{bath} = 50$ mK using Eq. (17) in Fig. D1.

We assume the QPs and the phonons to be of the same temperature and assume a Kapiza boundary on the interface between the TiN and the sapphire substrate as

$$P_d = \Sigma A_s (T_{qp}^4 - T_{bath}^4),$$

where ΣA_s is a material constant, and P is related to the power absorbed in the resonator[45] as

$$P_d = \eta_r \frac{P_r}{2} \frac{4Q^2}{Q_i Q_c} \frac{Q_i}{Q_{i,qp}} \quad (D.2)$$

where P_r is the readout power for the resonator, η_r is the fraction of the energy in the resonator that is dissipated, Q_i, Q_c, Q is the internal quality factor, the coupling quality factor, and the loaded quality factor respectively. $Q = Q_i Q_c / (Q_i + Q_c)$. We consider Q_i of the MKIDs to be dominated by the QPs and $Q_{i,qp} = Q_i$.

Thus, T_{qp} can be calculated as

$$T_{qp} = \left(\frac{\eta_r}{\Sigma A_s} \frac{P_r}{2} \frac{4Q^2}{Q_i Q_c} + T_{bath}^4 \right)^{1/4} \quad (D.3)$$

We set $\eta_r/\Sigma A_s$ as a fitting parameter and used Q_i and Q_c fitted from S_{21} to obtain T_{qp} .

We followed the procedure in the thesis by Coumou[55] to calculate the density of states of the QPs with the disorder α_d . We rewrite the Usadel equation Eq. 1 as

$$iE \sin \theta + \Delta \cos \theta - \alpha_d \sin \theta \cos \theta = 0$$

To calculate $\Delta(T)$, the Matsubara representation of these equations is used as

$$\Delta \cos \theta_n - \omega_n \sin \theta_n - \alpha \sin \theta_n \cos \theta_n = 0 \quad (\text{D.4})$$

with $\theta_n = \theta(\omega_n)$ and

$$\Delta \ln \left(\frac{T_c}{T} \right) = 2\pi k_B T \sum_{m=0}^{\infty} \left(\frac{\Delta}{\omega_m} - \sin \theta_n \right) \quad (\text{D.5})$$

Where $\omega_m = (2m+1)\pi k_B T$ are the Matsubara frequencies and $m = 0, 1, 2, \dots$. Eq. (D.4) and Eq. (D.5) need to be solved iteratively for all the frequencies until the convergence is reached. Once the $\Delta(T)$ is solved, $\sin \theta(E)$ and $\cos \theta(E)$ can be obtained from Eq. 1. With $\sin \theta(E)$ and $\cos \theta(E)$, the imagery part of complex conductivity $\sigma = \sigma_1 - j\sigma_2$ can be calculated with Eq. (3) as

$$\begin{aligned} \frac{\sigma_2}{\sigma_n} &= \int_{E_g - \hbar\omega}^{\infty} g_2(E, E') [1 - 2f(E')] dE \\ &+ \int_{E_g}^{\infty} g_2(E', E) [1 - 2f(E)] dE \end{aligned}$$

with $g_2 = \text{Im}\{\cos \theta(E)\} \text{Re}\{\cos \theta(E')\} + \text{Im}\{i \sin \theta(E)\} \text{Re}\{i \sin \theta(E')\}$, $E = E + \hbar\omega$ and E_g is effective energy gap with the DoS starts to be positive. With the calculated density of state $\rho(E) = N_0 \text{Re}(\cos(\theta(E)))$, the QP density in the superconductor can be calculated with Eq. (5) at T_{qp} as

$$\begin{aligned} n_T(T_{qp}) &= 2N_0 \int_{-\infty}^{\infty} f(E, T_{qp}) \rho(E, T_{qp}) dE, \\ n_{qp} &= \sqrt{\frac{\Gamma}{R} I + n_T^2} \end{aligned} \quad (\text{D.6})$$

With Eq. (11), $\tau_{qp} = \Gamma/(2n_{qp}R)$, and $\delta f/f = \alpha \delta \sigma_2 / 2\sigma_2$, τ_{qp} and the resonance frequency shift can be fitted together with $F_1 = \Gamma/R$, $F_2 = \eta_r/(\Sigma A_s)$, $F_3 = \alpha_d$ and $F_4 = I$ as the fitting parameters. We find $\gamma I/R$ is negligible.

Appendix E. Pulse fitting

In this section, we describe how we fit the single photon pulse response of MKIDs. We rewrite Eq.(21) for easy reference.

$$\begin{aligned} \frac{dn}{dt} &= D_{qp} \nabla^2 n + I + \beta P - Rn^2 \\ \frac{dP}{dt} &= D_{ph} \nabla^2 P - \beta P/2 + Rn^2/2 - \gamma(P - P_T^0) \end{aligned}$$

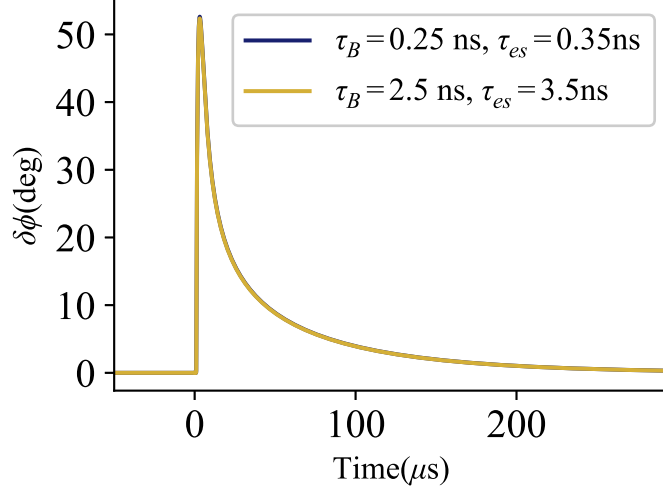


Figure E1. Comparison with simulation result with same β/γ but different β and γ

To solve Eq.(21), we need to know the D_{qp} , β , R , I and P_T^0 . From the fitting of τ_{qp} versus temperature, we have obtained value $F_1 = \Gamma/R$, which is

$$F_1 = (1 + \frac{\beta}{2\gamma})/R \quad (\text{E.1})$$

As long as we keep the same F_1 , the solution of Eq.(21) remains the same. This is reasonable as once F_1 is fixed, the τ_{qp} will be fixed with the same QP density. We assume that $\tau_{es} = 0.35$ ns and $\tau_B = 0.25$ ns to keep the β/γ on the order of 1 for both TiN_{1K} and TiN_{2K} as we don't observe R with our detector[10]. In Fig. E1, we show when the β/γ is kept the same, the solution is the same τ_{es} strongly depends on the acoustic mismatch between the superconductor and the substrate[56]. It is almost constant versus temperature[57]. We list the measured values τ_{es} of different commonly used superconductors for easy reference. For a film with a thickness of 60 nm, it is estimated to be 0.48 ns for niobium[57], around 0.5 ns for NbN depending on substrates[58], and 0.19 ns for aluminum on silicon[30]. τ_B is also considered a constant as its change can be negligible in the measured temperature range[56]. In this case, we obtain $\tau_0 = 248$ ns and 28 ns for TiN_{1K} and TiN_{2K} respectively, to be on the order of the measured values[50], which is calculated as[46]

$$\tau_0 = (\frac{2\Delta}{k_B T_c})^3 \frac{1}{4\Delta N_0 R} \quad (\text{E.2})$$

Here, we list the detailed parameters for fitting the pulse response in Table E1.

With the $P_T^0 = Rn_T^2/\beta$ calculated from Eq. (5), I fitted Appendix D, and an assumption that $D_{ph} = 0$, we can fit Eq.(21) for D_{qp} and the pair-breaking efficiency η with a proper initial condition.

Table E1. Parameters for pulse fitting for TiN_{1K} and TiN_{2K} @ $T_{bath} = 50$ mK

Parameters	TiN_{1K}	TiN_{2K}	comment
T_c	0.84 K	2.1 K	The critical temperature
α_d	0.12	0.092	The measure of the disorder of the flim
d	60 nm	15 nm	The film thickness
τ_B^a	0.25 ns	0.25 ns	The pair-breaking time
f_r	3.182 GHz	2.625 GHz	The resonance frequency
τ_0	248 ns	28 ns	The electron and phonon interaction time
τ_{es}^a	0.35 ns	0.35 ns	The phonon escape time
Q	6.3k	13.1k	The quality factor of the resonator.
V	78 μm^3	2.55 μm^3	The volume of the inductor.
R	$5.90 \times 10^{-18}\text{s}^{-1}$	$2.23 \times 10^{-17}\text{s}^{-1}$	The QP recombination rate
t_{qp}	121 mK	273 mK	The equivalent temperature of the QPs
σ_0^b	100 nm	60 nm	The variance of the initial QP distribution.

^a These two values are assumed to obtain the Γ . Then, by fitting the QP lifetime versus T_{bath} with Eq. (11), R can be obtained. τ_{es} for both films are kept the same for simplicity as we are not able to determine τ_{es} in both from our measurement.

^b The value is obtained to set η to be smaller than 0.6.

Appendix E.1. Initial Condition

The QPs generated by the absorbed photon in MKIDs is

$$\delta N_{qp} = \frac{\eta E_{ph}}{\Delta} \quad (\text{E.3})$$

where $E_{ph} = 3.06$ eV for a 405 nm photon.

We assume the QPs are Gaussian-distributed with σ_0 . Then, the initial density of the QPs as

$$\delta N_{qp} = wd \int_{-l/2}^{l/2} \frac{1}{\sigma_0 \sqrt{2\pi}} e^{-\frac{x^2}{2\sigma_0^2}} dx \quad (\text{E.4})$$

where w is the width of the strip, d is the film thickness and l is the length of the meander. The Gaussian distribution is taken for simplicity as the QP density should be continuous and symmetrical after the initial photon absorption, meanwhile it is a good approximation to the Dirac function.

Appendix E.2. 1D-Diffusive RT equation

We solve the 1D-Diffusive RT equation for n_{qp} and keep only η and D_{qp} as the fitting parameter. We show the fitting χ^2 for the pulse TiN_{2K} at $T_{bath} = 50$ mK in Fig. E2.

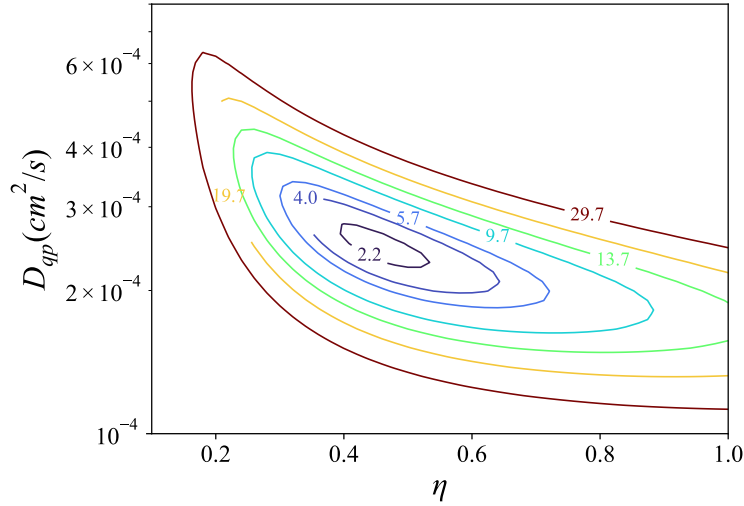


Figure E2. Fitting χ^2 for TiN_{2K} at $T_{bath} = 50$ mK

References

- [1] Leduc H G, Bumble B, Day P K, Eom B H, Gao J, Golwala S, Mazin B A, McHugh S, Merrill A, Moore D C, Noroozian O, Turner A D and Zmuidzinas J 2010 *Applied Physics Letters* **97** 102509 ISSN 0003-6951 URL <http://aip.scitation.org/doi/abs/10.1063/1.3480420>
- [2] Mazin B A, Meeker S R, Strader M J, Szypryt P, Marsden D, van Eyken J C, Duggan G E, Walter A B, Ulbricht G, Johnson M, Bumble B, O'Brien K and Stoughton C 2013 *Publications of the Astronomical Society of the Pacific* **125** 1348 URL <https://dx.doi.org/10.1086/674013>
- [3] Bueno J, Coumou P C J J, Zheng G, de Visser P J, Klapwijk T M, Driessen E F C, Doyle S and Baselmans J J A 2014 *Applied Physics Letters* **105** 192601 ISSN 0003-6951 1077-3118
- [4] Zobrist N, Coiffard G, Bumble B, Swimmer N, Steiger S, Daal M, Collura G, Walter A B, Bockstiegel C, Fruitwala N, Lipartito I and Mazin B A 2019 *Applied Physics Letters* **115** 213503 URL <https://doi.org/10.1063/1.5127768>
- [5] Chang J B, Vissers M R, Córcoles A D, Sandberg M, Gao J, Abraham D W, Chow J M, Gambetta J M, Beth Rothwell M, Keefe G A, Steffen M and Pappas D P 2013 *Applied Physics Letters* **103** 012602 ISSN 0003-6951 URL <https://doi.org/10.1063/1.4813269>
- [6] Day P K, LeDuc H G, Mazin B A, Vayonakis A and Zmuidzinas J 2003 *Nature* **425** 817–821 ISSN 1476-4687 URL <https://doi.org/10.1038/nature02037>
- [7] Gao J, Vissers M R, Sandberg M O, da Silva F C S, Nam S W, Pappas D P, Wisbey D S, Langman E C, Meeker S R, Mazin B A, Leduc H G, Zmuidzinas J and Irwin K D 2012 *Applied Physics Letters* **101** 142602 ISSN 0003-6951 1077-3118
- [8] Guo W, Liu X, Wang Y, Wei Q, Wei L F, Hubmayr J, Fowler J, Ullom J, Vale L, Vissers M R and Gao J 2017 *Applied Physics Letters* **110** 212601 ISSN 0003-6951 1077-3118
- [9] de Visser P J, Baselmans J J, Bueno J, Llombart N and Klapwijk T M 2014 *Nat Commun* **5** 3130 ISSN 2041-1723 (Electronic) 2041-1723 (Linking) URL <https://www.ncbi.nlm.nih.gov/pubmed/24496036>
- [10] Zobrist N, Clay W H, Coiffard G, Daal M, Swimmer N, Day P and Mazin B A 2022 *Physical Review Letters* **129** 017701
- [11] Hubmayr J, Beall J, Becker D, Cho H M, Devlin M, Dober B, Groppi C, Hilton G C, Irwin K D, Li D, Mauskopf P, Pappas D P, Van Lanen J, Vissers M R, Wang Y, Wei L F and Gao J 2015 *Applied Physics Letters* **106** 073505 ISSN 0003-6951 1077-3118
- [12] Bardeen J, Cooper L N and Schrieffer J R 1957 *Physical Review* **108** 1175–1204 URL [http:](http://)

- [//link.aps.org/doi/10.1103/PhysRev.108.1175](https://link.aps.org/doi/10.1103/PhysRev.108.1175)
- [13] Boussaha F, Hu J, Nicaise P, Martin J M, Chaumont C, Dung P V, Firminy J, Reix F, Bonifacio P, Piat M and Geoffray H 2023 *Applied Physics Letters* **122** ISSN 0003-6951 1077-3118
 - [14] Jie H, Paul N, Faouzi B, Jean-Marc M, Christine C, Alexine M, Florent R, Josiane F, Thibaut V, Dung P V, Michel P, Elisabetta C and Piercarlo B 2024 *Journal of Low Temperature Physics* **214** 113–124 ISSN 1573-7357 URL <https://doi.org/10.1007/s10909-023-03018-5>
 - [15] Driessen E F C, Coumou P C J J, Tromp R R, de Visser P J and Klapwijk T M 2012 *Physical Review Letters* **109** 107003 URL <http://link.aps.org/doi/10.1103/PhysRevLett.109.107003>
 - [16] Rothwarf A and Taylor B N 1967 *Physical Review Letters* **19** 27–30 ISSN 0031-9007
 - [17] Beldi S, Boussaha F, Hu J, Monfardini A, Traini A, Levy-Bertrand F, Chaumont C, Gonzales M, Firminy J, Reix F, Rosticher M, Mignot S, Piat M and Bonifacio P 2019 *Opt Express* **27** 13319–13328 ISSN 1094-4087 (Electronic) 1094-4087 (Linking) URL <https://www.ncbi.nlm.nih.gov/pubmed/31052858>
 - [18] de Visser P J, de Rooij S A, Murugesan V, Thoen D J and Baselmans J J 2021 *Phys. Rev. Applied* **16**(3) 034051 URL <https://link.aps.org/doi/10.1103/PhysRevApplied.16.034051>
 - [19] Hu J, Boussaha F, Martin J M, Nicaise P, Chaumont C, Beldi S, Piat M and Bonifacio P 2021 *Applied Physics Letters* **119** ISSN 0003-6951 1077-3118
 - [20] Nicaise P, Hu J, Martin J M, Beldi S, Chaumont C, Bonifacio P, Piat M, Geoffray H and Boussaha F 2022 *Journal of Low Temperature Physics* **209** 1242–1248 ISSN 1573-7357 URL <https://doi.org/10.1007/s10909-022-02789-7>
 - [21] Coumou P C J J, Driessen E F C, Bueno J, Chapelier C and Klapwijk T M 2013 *Physical Review B* **88** ISSN 1098-0121 1550-235X
 - [22] Lyu W T, Zhi Q, Hu J, Li J and Shi S C 2023 *Chinese Physics B* URL <http://iopscience.iop.org/article/10.1088/1674-1056/ad03dc>
 - [23] Nam S B 1967 *Physical Review* **156** 487–493 URL <https://link.aps.org/doi/10.1103/PhysRev.156.487>
 - [24] Twerenbold D 1986 *Phys Rev B Condens Matter* **34** 7748–7759 ISSN 0163-1829 (Print) 0163-1829 (Linking) URL <https://www.ncbi.nlm.nih.gov/pubmed/9939456>
 - [25] Lindgren M, Currie M, Williams C, Hsiang T, Fauchet P, Sobolewski R, Moffat S, Hughes R, Preston J and Hegmann F 1999 *Applied Physics Letters* **74** 853–855
 - [26] Demsar J, Averitt R D, Taylor A J, Kabanov V V, Kang W N, Kim H J, Choi E M and Lee S I 2003 *Phys Rev Lett* **91** 267002 ISSN 0031-9007 (Print) 0031-9007 (Linking) URL <https://www.ncbi.nlm.nih.gov/pubmed/14754080>
 - [27] Kabanov V V, Demsar J and Mihailovic D 2005 *Phys Rev Lett* **95** 147002 ISSN 0031-9007 (Print) 0031-9007 (Linking) URL <https://www.ncbi.nlm.nih.gov/pubmed/16241687>
 - [28] Beck M, Klammer M, Lang S, Leiderer P, Kabanov V V, Gol'Tsman G and Demsar J 2011 *Physical Review Letters* **107** 177007
 - [29] Sacepe B, Chapelier C, Baturina T I, Vinokur V M, Baklanov M R and Sanquer M 2008 *Phys Rev Lett* **101** 157006 ISSN 0031-9007 (Print) 0031-9007 (Linking) URL <https://www.ncbi.nlm.nih.gov/pubmed/18999631>
 - [30] de Rooij S 2020 *Quasiparticle Dynamics in Optical MKIDs: Single Photon Response and Temperature Dependent Generation-Recombination Noise* Master thesis TU Delft
 - [31] Wilson C M and Prober D E 2004 *Physical Review B* **69** ISSN 1098-0121 1550-235X
 - [32] Wang C, Gao Y Y, Pop I M, Vool U, Axline C, Brecht T, Heeres R W, Frunzio L, Devoret M H, Catelani G, Glazman L I and Schoelkopf R J 2014 *Nat Commun* **5** 5836 ISSN 2041-1723 (Electronic) 2041-1723 (Linking) URL <https://www.ncbi.nlm.nih.gov/pubmed/25518969>
 - [33] Kozorezov A G, Volkov A F, Wigmore J K, Peacock A, Poelaert A and den Hartog R 2000 *Physical Review B* **61** 11807–11819 pRB URL <https://link.aps.org/doi/10.1103/PhysRevB.61.11807>
 - [34] Zmuidzinas J 2012 *Annual Review of Condensed Matter Physics* **3** 169–214 ISSN 1947-5454 URL <http://dx.doi.org/10.1146/annurev-conmatphys-020911-125022>

- [35] Martinez M, Cardani L, Casali N, Cruciani A, Pettinari G and Vignati M 2019 *Physical Review Applied* **11** ISSN 2331-7019
- [36] Kouwenhoven K, Fan D, Biancalani E, de Rooij S A, Karim T, Smith C S, Murugesan V, Thoen D J, Baselmans J J and de Visser P J 2022 *arXiv preprint arXiv:2207.05534* URL <https://arxiv.org/abs/2207.05534>
- [37] Fyhrie A, Zmuidzinas J, Glenn J, Day P, LeDuc H G and McKenney C 2018 Progress towards ultra sensitive kids for future far-infrared missions: a focus on recombination times vol 10708 ed Zmuidzinas J and Gao J R International Society for Optics and Photonics (SPIE) p 107083A URL <https://doi.org/10.1117/12.2312867>
- [38] Barends R, Baselmans J J, Yates S J, Gao J R, Hovenier J N and Klapwijk T M 2008 *Phys Rev Lett* **100** 257002 ISSN 0031-9007 (Print) 0031-9007 (Linking) URL <https://www.ncbi.nlm.nih.gov/pubmed/18643694>
- [39] Vissers M R, Gao J, Wisbey D S, Hite D A, Tsuei C C, Corcoles A D, Steffen M and Pappas D P 2010 *Applied Physics Letters* **97** 232509 ISSN 0003-6951 1077-3118
- [40] Hu J, Salatino M, Traini A, Chaumont C, Boussaha F, Goupil C and Piat M 2020 *Journal of Low Temperature Physics* **199** 355–361 ISSN 1573-7357 URL <https://doi.org/10.1007/s10909-019-02313-4>
- [41] Narayanamurti V, Dynes R C, Hu P, Smith H and Brinkman W F 1978 *Physical Review B* **18** 6041–6052 URL <https://link.aps.org/doi/10.1103/PhysRevB.18.6041>
- [42] Mattis D C and Bardeen J 1958 *Physical Review* **111** 412–417 URL <http://link.aps.org/doi/10.1103/PhysRev.111.412>
- [43] Gao J, Zmuidzinas J, Vayonakis A, Day P, Mazin B and Leduc H 2008 *Journal of Low Temperature Physics* **151** 557–563 ISSN 0022-2291 1573-7357
- [44] Pollack G L 1969 *Reviews of Modern Physics* **41** 48–81 rMP URL <https://link.aps.org/doi/10.1103/RevModPhys.41.48>
- [45] de Visser P J, Goldie D J, Diener P, Withington S, Baselmans J J and Klapwijk T M 2014 *Phys Rev Lett* **112** 047004 ISSN 1079-7114 (Electronic) 0031-9007 (Linking) URL <https://www.ncbi.nlm.nih.gov/pubmed/24580483>
- [46] Guruswamy T 2018 *Nonequilibrium behaviour and quasiparticle heating in thin film superconducting microwave resonators* Ph.d. thesis University of Cambridge
- [47] Thomas C N, Withington S, Sun Z, Skyrme T and Goldie D J 2020 *New Journal of Physics* **22** 073028 ISSN 1367-2630
- [48] Budoyo R P, Hertzberg J B, Ballard C J, Voigt K D, Kim Z, Anderson J R, Lobb C J and Wellstood F C 2016 *Physical Review B* **93** ISSN 2469-9950 2469-9969
- [49] Rajauria S, Courtois H and Pannetier B 2009 *Physical Review B* **80** ISSN 1098-0121 1550-235X
- [50] Kardakova A, Finkel M, Morozov D, Kovalyuk V, An P, Dunscombe C, Tarkhov M, Mauskopf P, Klapwijk T M and Goltsman G 2013 *Applied Physics Letters* **103** ISSN 0003-6951 1077-3118
- [51] Martinis J M, Ansmann M and Aumentado J 2009 *Phys Rev Lett* **103** 097002 ISSN 0031-9007 (Print) 0031-9007 (Linking) URL <https://www.ncbi.nlm.nih.gov/pubmed/19792820>
- [52] Escoffier W, Chapelier C, Hadacek N and Villégier J C 2004 *Phys. Rev. Lett.* **93**(21) 217005 URL <https://link.aps.org/doi/10.1103/PhysRevLett.93.217005>
- [53] Vodolazov D Y 2017 *Physical Review Applied* **7** ISSN 2331-7019
- [54] Mazin B A 2005 *Microwave kinetic inductance detectors* Ph. d thesis California Institute of Technology
- [55] Coumou P C J J 2015 *Electrodynamics of strongly disordered superconductors* Ph. d thesis TU Delft, Delft University of Technology
- [56] Kaplan S B, Chi C C, Langenberg D N, Chang J J, Jafarey S and Scalapino D J 1976 *Physical Review B* **14** 4854–4873 URL <https://link.aps.org/doi/10.1103/PhysRevB.14.4854>
- [57] Oktasendra F, Berdiyrov G, Mekki A and Maneval J 2016 *IEEE Transactions on Applied Superconductivity* **26** 1–4 ISSN 1051-8223
- [58] Sidorova M, Semenov A, Hübers H W, Ilin K, Siegel M, Charaev I, Moshkova M, Kaurova N,

Goltsman G N and Zhang X 2020 *Physical Review B* **102** 054501